

THE PENNSYLVANIA STATE UNIVERSITY  
SCHREYER HONORS COLLEGE

DEPARTMENT OF BIOCHEMISTRY AND MOLECULAR BIOLOGY

PURIFICATION AND CHARACTERIZATION OF A RECOMBINANT SMALL SUBUNIT OF THE  
MEMBRANE-BOUND HYDROGENASE OF *RALSTONIA EUTROPHA*: TOWARDS  
CONSTRUCTION OF A PHOTOCHEMICAL H<sub>2</sub>-PRODUCING MODULE

IAN PRICE  
Spring 2010

A thesis  
submitted in partial fulfillment  
of the requirements  
for a baccalaureate degree  
in Biochemistry and Molecular Biology  
with honors in Biochemistry and Molecular Biology

Reviewed and approved\* by the following:

John H. Golbeck  
Professor of Biochemistry and Molecular Biology, Professor of Chemistry  
Thesis Supervisor

Joseph C. Reese  
Professor of Biochemistry and Molecular Biology  
Honors Adviser

Scott Selleck, Department Head  
Department of Biochemistry and  
Molecular Biology

\* Signatures are on file in the Schreyer Honors College.

**ABSTRACT:**

In recent decades, there has been an increased interest in utilizing the process of photosynthesis to help solve humans' energy needs, both *in* and *ex vivo*. Concurrently, interest has grown in hydrogen as a major component of the energy economy. Many methods of utilizing the high quantum yield and energy efficiency evolved in the photosynthetic complexes of cyanobacteria or plants have been proposed. One method developed in this laboratory involves the direct coupling of a photosystem I complex to an exogenous catalyst (synthetic or proteinaceous) via a so-called "molecular wire". This approach generally involves a modified hydrocarbon artificially inserted into the electron transport chain of photosystem on one end and attached to the catalyst on the other end. Hydrogen production via such substitution has been demonstrated in earlier modules in the Golbeck lab.

Hydrogenase enzymes are clear choices for biological catalysts of the ( $2\text{H}^+ + 2\text{e}^- \rightarrow \text{H}_2$ ) half reaction in the production of hydrogen. The [NiFe] hydrogenases have garnered particular interest for such use in hydrogen production due to their resistance to irreversible inactivation by oxygen ( $\text{O}_2$ ). [NiFe] hydrogenases are heterodimeric, with a large subunit that contains the [NiFe] active site and a small subunit that contains an electron transport chain with two [4Fe-4S] clusters and a [3Fe-4S] cluster. In particular, the [NiFe] hydrogenases of the Knallgas bacteria, including the genus *Ralstonia*, are of interest because of their ability not just to resist permanent  $\text{O}_2$  damage, but to retain their reversible  $\text{H}_2$ -oxidizing activity at atmospheric  $\text{O}_2$  levels.

Here, a recombinant form of the small subunit of the membrane-bound hydrogenase of *Ralstonia eutropha* has been engineered to contain an open coordination site in the distal

[4Fe-4S] cluster in the electron transport chain (His 187 converted to a Gly). Said protein has been cloned into and overexpressed in *Escherichia coli*, without the large subunit. Several purification schemes were evaluated to overcome the persistent insolubility of HoxK (small subunit). Electron transport-associated iron-sulfur clusters were reconstituted by an accepted protocol. Electron paramagnetic resonance spectroscopic analysis confirmed the formation of iron-sulfur clusters and may suggest the recruitment of an exogenous ligand (2-mercaptoethanol) into the missing coordination site of the distal iron-sulfur cluster. This construction, along with reconstituted active large subunit, could constitute part of an effective photochemical module for the *ex vivo* synthesis of H<sub>2</sub> via coupling to a photosystem I by means of the “molecular wire” method described.

Purification methods used for the other proteins necessary for the photochemical module suggested are also provided. *Synechococcus* sp. PCC 7002 PsaC molecular-wire mutant has been constructed from *E. coli*-expressed protein and the *Synechococcus* PCC 7002 photosystem I from the native cyanobacteria.

## TABLE OF CONTENTS:

Introduction .....	1
Methods.....	14
Results.....	20
Discussion.....	28
Acknowledgements.....	33
References.....	34
Appendices:	
A. DNA and Protein Sequences.....	39
B. Solutions and Protocols.....	41
C. Additional Purification Methods .....	42
D. Additional EPR Spectra.....	44
Academic Vitae	

## INTRODUCTION:

### **The Place of Hydrogen in an Evolving Energy Economy**

In light of recent trends in energy costs, pollution, climate change, and technological advances, the appeal of hydrogen ( $H_2$ ) as a fuel has risen. The major advantage of hydrogen is its cleanliness: the only product of its combustion is water. Additionally, a diversity in energy supply is desirable for a sustainable energy economy. To this end, the use of hydrogen as an energy carrier would lend itself to production from various energy sources (e.g. wind, tidal, nuclear, and solar), many of which are renewable sources.

As with other new alternative energy systems, a hydrogen fuel energy system does present significant logistical challenges. These include dangers arising from its flammability, the costs of new infrastructure, and low energy density. (Though hydrogen contains roughly three times as much usable energy as gasoline by mass, it contains less than one-fourth as much energy by volume, as a liquid or compressed gas.) (16). Furthermore, the most significant current means of industrial hydrogen production involves energy-inefficient conversion of fossil fuel hydrocarbons.

Thus, advances in technology are necessary for the realistic implementation of hydrogen as a major player in the energy economy. These include inexpensive storage and delivery systems, which are the subject of much promising research. Importantly, the cost- and energy-efficiency of hydrogen production from renewable sources must also be improved.

### **Photosynthesis: The Original Photochemical Energy Conversion Nanomachine**

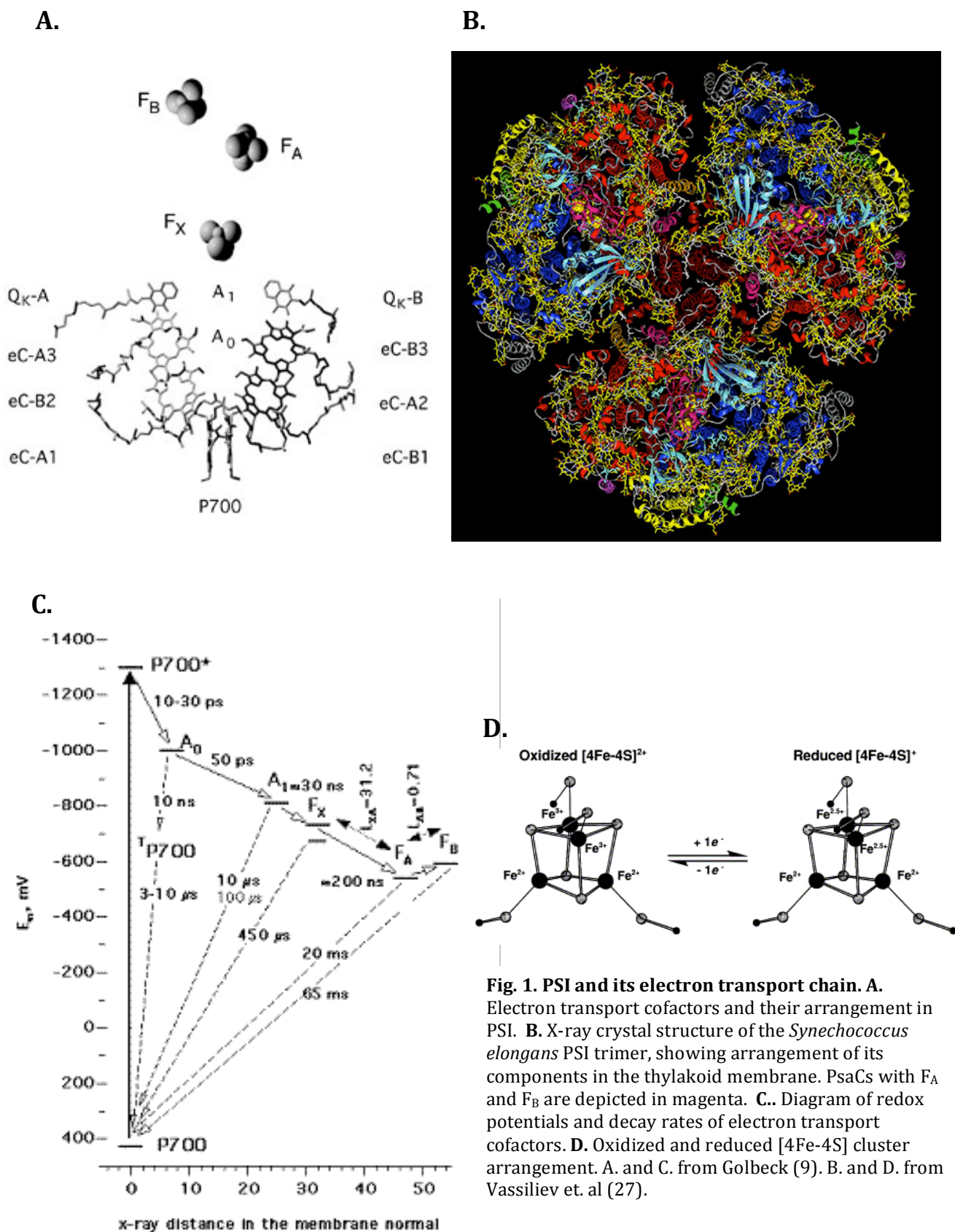
Due to the widespread and abundant nature of sunlight, solar energy deserves attention for application to various energy needs. Though there has been significant

improvement in synthetic photovoltaic devices to capture the energy available in solar photons, none has been able to approach the efficiency of the exquisite machinery evolved in photosynthetic organisms (16).

In plants and cyanobacteria, two classes of thylakoid membrane-integral complexes called reaction centers (RCs) capture the energy in visible photons for use in chemical reactions. These are called photosystems I and II (PSI and PSII). The first RC, PSII is responsible for the splitting of water via the half-redox reaction ( $\text{H}_2\text{O} + 2h\nu \rightarrow 2\text{H}^+ + \frac{1}{2}\text{O}_2 + 2\text{e}^-$ ), in which protons are built up on one side of the membrane (9). ATP synthase utilizes the resulting electrochemical gradient to create high-energy phosphate bonds in ATP. Two of the (now lower-potential) electrons from the water-splitting reaction are conveyed to the terminal electron acceptor of PSII,  $\text{Q}_\text{B}$  forming  $\text{Q}_\text{B}\text{H}_2$ , a mobile plastoquinone (30). These electrons continue through a cytochrome  $\text{b}_6\text{f}$  complex to a plastocyanin, eventually to a PSI (see Fig 1).

Each RC includes an extensive network of photon-absorbing and energy-transferring molecules. Specifically, these antennae include chlorophylls and carotenoids. In both PSI and PSII, photon energy absorbed by the chlorophylls is passed to a “special pair” of chlorophylls, in which it excites an electron enough to create a charge-separated state (16) In order to avoid charge recombination, an electron transport chain transfers the electron away from the special pair through the complex across the membrane, leaving a hole on the special pair. This hole must be reduced (usually within the  $\mu\text{s}$ -ms range) (9). For PSII, these electrons come from a manganese-containing metal cluster, which in turn gets them from water. In PSI, the direct electron source is the reduced mobile plastocyanin, which associates on the luminal side of PSI (see Fig. 1A).

Effectively, in PSI light excites an electron from a potential of about +340 mV (plastocyanin) to about -580 mV in the distal [4Fe-4S] cluster cofactor of the PSI electron transport chain (see Fig. 1B, C) (19). The electron transport chain of PSI, after the special pair, P700, bifurcates into an A and a B branch, each containing another chlorophyll (e.g. A<sub>0</sub>) and a phylloquinone (A<sub>1</sub>). Three [4Fe-4S] clusters (F<sub>x</sub>, F<sub>a</sub>, and F<sub>B</sub>) finish the chain. All of the cofactors through F<sub>x</sub> are located in the membrane-integral PsaA/B proteins. F<sub>A</sub> and F<sub>B</sub> are in the associated PsaC subunit (27). Electron transport is known to pass through the A branch in cyanobacteria. The involvement of the B branch has been debated, but several techniques, including high-frequency EPR data, suggest that the B branch is active to an extent as well, (20). Fig. 1D shows the redox potentials of the PSI electron transport chain cofactors. The important accomplishment of PSI is the long-lasting (~60 ms) charge separated state P700<sup>+</sup>/F<sub>B</sub><sup>-</sup>, which allows the reduction of an external electron acceptor. Physiologically, electrons most often are transferred from F<sub>B</sub> to a soluble ferredoxin or flavodoxin protein (see Fig. 1A) (9). These low-potential electrons are eventually used to reduce an NADP<sup>+</sup> to an NADPH via the overall half reaction of  $(2e^- + H^+ + NADP^+ \rightarrow NADPH)$ . The reduced F<sub>B</sub> cluster (about -580 mV) of PsaC is of interest in this study, as it provides a site for electron transfer to an artificial acceptor with H<sup>+</sup>-reducing catalytic activity.





Using this method of coupling type II and type I RCs, cyanobacteria and plants are able to build up oxidizing potential to oxidize water and enough reducing potential to reduce  $\text{NADP}^+$  to NADPH, which can then be used for the dark reactions or directly in metabolism. It is this great reducing power derived from abundant visible photons that makes the cyanobacterial/plant photosynthetic system attractive for human energy needs. With clever engineering, the electrons leaving PSI may have the potential (no pun intended) to be coupled to various chemical reactions or to create electrical current. The chemistry, physics, and molecular biology involved in these type I RCs have been the subject of many research projects in the Golbeck lab.

Due to this background, and because PSI produces such a strong reductant with solar energy, our current research is designed to incorporate PSI in the second half-reaction in the synthesis of dihydrogen in a new catalytic module.

PSI is well suited chemically to the reduction of protons to form  $\text{H}_2$ . NADPH has been described as the biological equivalent of  $\text{H}_2$ , as they have similar potentials ( $E'_0 = -324$  and  $-414$  mV, respectively) (17). Both of these are higher than that of  $\text{F}_\text{B}$ , meaning there is sufficient reducing power to make hydrogen. In addition to having a compatible redox potential, PSI has evolved a very high quantum yield, effectively 1.0. (Quantum yield is the ratio of photons that successfully lead to a  $\text{P700}^+/\text{F}_\text{B}^-$  charge-separated state to the total number of photons absorbed). The 96 chlorophylls and 22 carotenes in PSI's antenna system also cover a large area of absorption, and absorb a large range of wavelengths (all visibles below 700 nm) (16). Thus, not only do PSI RCs create a stable high-energy reductant, but they do so with high efficiency and a large optical cross-section. This reaction surpasses the efficiency of any synthetic photovoltaic cells to date.

## Direct Coupling of RCs

In designing systems utilizing the photosynthetic molecular machinery for energy capture, the coupling of the photon-absorbing electron donor (like PSI) to the reduction catalyst is one of the main areas of research. If electron transfer is left up to diffusion in solution, low rates and efficiency are likely due to rate-limiting diffusion kinetics (Golbeck). Various methods of electrically connecting PSI and catalyst have been attempted. Such methods have included precipitation on conductors and the creation of fusion proteins (12)

One novel method of directly coupling a protein's electron transport chain to another catalyst is by a so-called "molecular wire." The Golbeck lab has previously demonstrated applications of this method of facilitating the transport of the low-potential electron from PSI (11). The "molecular wire" method is the subject of several concurrent projects, including this one. (Another project is attempting to use the PSI to power a nitrogenase to create reduced nitrogen compounds) (Golbeck, unpublished data). Specifically, I helped with projects wiring the PsaC subunit of the PSI complex.

In the molecular wire method, a coordination ligand of a surface-located electron transport site (e.g. an iron-sulfur cluster) is removed from the protein, and a modified hydrocarbon "tether" molecule is substituted into the site via a functional group on its end. In PsaC, cysteine 14, which coordinates the [4Fe-4S]  $F_B$  cluster, is changed to a glycine (see Fig. 2). (In addition, it was found that converting cysteine 34, near the iron-sulfur cluster, aids in cluster formation, possibly for steric reasons.) When the recombinant proteins are overexpressed in *E. coli*, the iron-sulfur clusters must be reconstituted, as most are not compatible with the *E. coli* maturation systems. Fortunately, this has so far proven successful by incubation with excess  $Fe^{2+}$  and  $S^{2-}$  under reducing, anaerobic conditions. In

reconstitution, excess 2-mercaptoethanol can serve to provide reducing conditions and as a replacement “rescue” sulfide ligand to Fe-S clusters. Subsequent to Fe-S reconstitution, a molecular wire with a sulfide group at the end can be used to displace the rescue ligand.

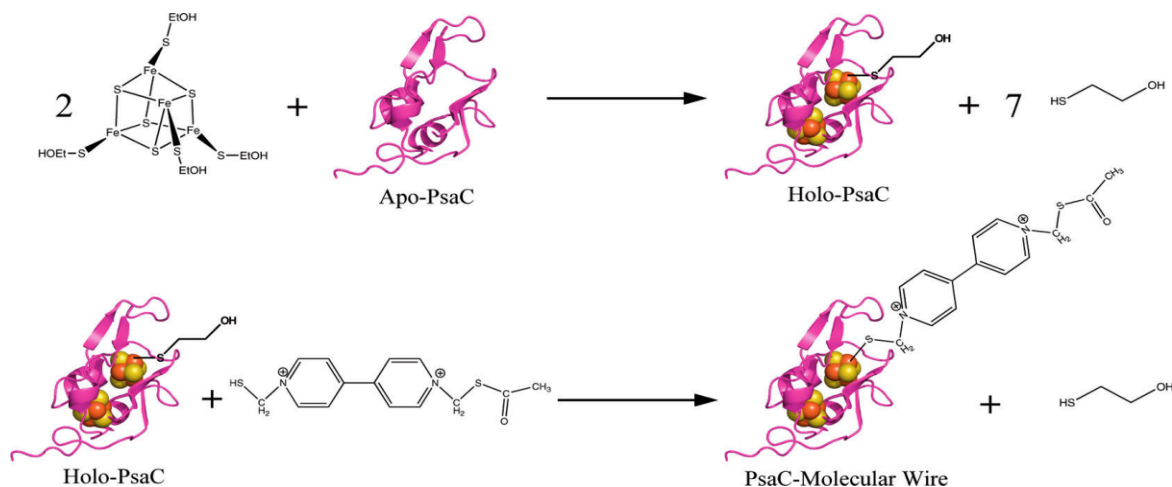


**Fig. 2. The molecular wire method on a PsaC C13G/C33S mutant.** Fe-S clusters are rebuilt and put into PsaC in the presence of 2-mercaptoethanol, which acts as a “rescue ligand”. A thiol on the wire then displaces the 2-mercaptoethanol at the Fe-S cluster. Here, the wire is 1-(3-thiopropyl)-10-[3-(acetylthio)propyl]-4,40-bipyridinium. From Lubner et. al. (17).

Interestingly, wiring of PSI has also been demonstrated by extraction of the phylloquinone (see Fig. 1) in the electron transport chain and subsequent substitution with a naphthoquinone-viologen tether to a gold surface (26).

The molecular wiring of PsaC, as shown in Fig. 2, has been demonstrated with catalytic activity by the Golbeck lab in the formation of H<sub>2</sub>-producing bioconjugates. Namely, gold and platinum nanoparticles have showed impressive rates of H<sub>2</sub> evolution (11). I have been involved with the protein purification and analysis in several of these earlier projects involving PsaC and other PSI-related proteins. Though nanoparticles have been demonstrated successfully, optimization of H<sub>2</sub> production is ongoing. Among molecular wires used are bipyridinium (as in Fig. 2) and dithiol alkyl chains (17). The physics of electron transport along these chains is not yet clear. Originally, it was thought

that the electron would travel through the conjugated bonds of the tether. However, success with tethers lacking these bonds (e.g. 1,6-hexanedithiol) suggests it may quantum mechanically tunnel to the next cofactor due to its increased proximity (17). This may suggest other possible ways of wiring the reactants, but these are not discussed here.

## **The Hydrogenases**

Hydrogenases, which catalyze the reversible reaction ( $\text{H}_2 \leftrightarrow 2 \text{H}^+ + 2\text{e}^-$ ) are naturally of interest in  $\text{H}_2$  producing bioconjugates. There are three main types of hydrogenase in nature: iron-iron, nickel-iron, and iron (16). Iron, or [Fe]-hydrogenases contain a single iron in their enzymatic active site and occur often in methanogens. These hydrogenases are light-sensitive and thus would not be appropriate in photocatalysis (17). Iron-iron hydrogenases, as suggested, contain a di-iron [FeFe] active site. [FeFe] hydrogenases are physiologically bidirectional, but predominantly produce  $\text{H}_2$ . Though they generate  $\text{H}_2$  at high rates, [FeFe] hydrogenases are irreversibly inactivated by  $\text{O}_2$ . The third class, [NiFe] hydrogenases, contain [NiFe] active sites and are physiologically  $\text{H}_2$ -consuming. However, they are generally more  $\text{O}_2$ -tolerant. Though the majority are also inactivated by  $\text{O}_2$ , inactivation is mostly reversible (18). “Knallgasbacteria”, which use hydrogen in oxic conditions, are unique in that they produce hydrogenases that are highly resistant to this inactivation (16). (The name “knallgas” roughly translates from Swedish as “bang gas”, alluding to their habitation in  $\text{H}_2$ - and  $\text{O}_2$ -containing environments.) (22).

## **The $\text{O}_2$ -Tolerant *Ralstonia eutropha* Membrane-Bound Hydrogenase**

*Ralstonia eutropha*, strain H16 (formerly *Alcaligenes eutrophus*) is a Gram-negative, chemolithoautotrophic  $\beta$ -proteobacterium found in both soil and fresh water (22). Though it is strictly respiratory, it has been noted for its ability to use various electron donors and

acceptors, in both aerobic and anaerobic conditions. It can also fix CO<sub>2</sub> and store carbon as a bio-polymer in poly[R-(-)-3-hydroxybutyrate]. As a member of the knallgas bacteria, *R. eutropha* can metabolize hydrogen while still using O<sub>2</sub> as a terminal electron acceptor. Indeed, it is capable of living with H<sub>2</sub> as its sole energy source, at ambient O<sub>2</sub> levels. To fit this niche, knallgas bacteria have evolved oxygen-tolerant uptake hydrogenases, which each have different methods of O<sub>2</sub>-resistance. Involved in the hydrogen-oxidation of *R. eutropha* are three [NiFe] O<sub>2</sub>-tolerant hydrogenases: a cytoplasmic, soluble hydrogenase (SH), a periplasmically-oriented membrane-bound hydrogenase (MBH), and a regulatory hydrogenase (RH) (4). The SH and MBH are both involved in H<sub>2</sub> uptake, using the H<sub>2</sub> as an electron source to reduce NAD<sup>+</sup> for metabolic use. The RH is responsible for H<sub>2</sub>-sensing, and it is linked to regulation of the genes for SH and MBH.

The MBH, the subject of this study, contains two subunits. A 67.1-kDa large subunit (HoxG) contains the [NiFe] active site. The 34.6-kDa small subunit (HoxK) coordinates one [3Fe-4S] and two [4Fe-4S] clusters. The large-small subunit heterodimer binds via a C-terminal extension of HoxK to HoxZ, a b-type cytochrome, on the periplasmic side of the cell membrane. Importantly, though the physiological reaction of MBH is H<sub>2</sub> oxidation, it is reversible, as a true enzyme. Indeed, the bidirectionality of hydrogenases in *R. eutropha* serves as a protective outlet from excess reducing NADPH in the cell (15,16) . See Fig. 3 for the structure of MBH.

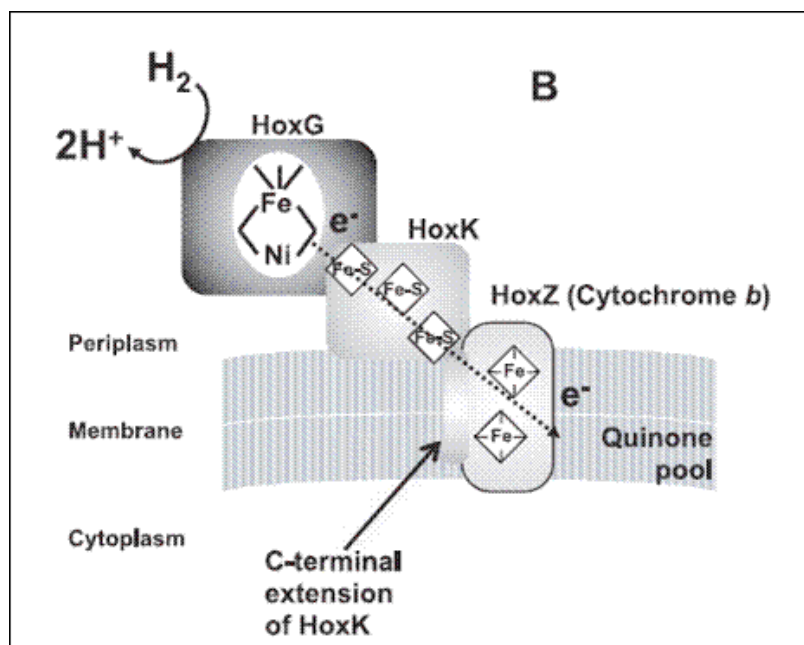


**Fig. 3. The membrane-bound hydrogenase (MBH) of *R. eutropha*.** From Saggu, et. al. (23).

No crystal structure is yet available for MBH. Thus, other techniques have been used to elucidate its structure. Electron paramagnetic resonance spectroscopy (EPR), used in this study, has proved a powerful method for examining the active site and electron transport chain, as it only “looks” at species with unpaired electron spins. Titrations and EPR measurements have determined the midpoint redox potentials of the electron transport cofactors at pH 7.0 (see table 1) (4, 13).

Cofactor	Location	Midpoint Potential, $E_{m7}$ (mV)
[NiFe]	HoxG	-110 (Ni)
Proximal [4Fe-4S]	HoxK	-180
Medial [3Fe-4S]	HoxK	+25
Distal [4Fe-4S]	HoxK	-60

**Table 1. Midpoint Redox potentials of the electron transport cofactors of MBH.** Data from Cramm (4).

The positive O<sub>2</sub>-tolerance of MBH is the reason for its use here, and is subject of much study. In SH, a narrow gas channel leading to the active site confers O<sub>2</sub> tolerance by restricting reaction with O<sub>2</sub>. Though there is no structural information, the MBH dimer's active site appears conserved with those of known anaerobic [NiFe] hydrogenases (23). The amino acid sequence at the active sites of O<sub>2</sub> tolerant [NiFe] hydrogenases is the same as those of standard [NiFe] hydrogenases, and IR spectra show similar arrangement of CO<sup>-</sup> and CN<sup>-</sup> ligands at the [NiFe] cluster as well. Thus, the oxygen-tolerance of the MBH must be due to other factors. As opposed to “standard” (i.e. O<sub>2</sub>-inactivated) [NiFe] hydrogenases, no Ni(III) “unready-inactive” (Ni<sub>u</sub>-A) is observed in EPR of *Ralstonia* MBH, even when exposed to O<sub>2</sub> (18).

The medial [3Fe-4S] cluster has a higher potential than either of the [4Fe-4S] clusters. This would seem counter-intuitive if it is part of the electron transport chain, as it would imply an uphill electron transfer. However, transfer through the proximal cluster is possible due to the overall negative Gibbs free energy of the transfer. EPR spectra of the proximal [4Fe-4S] cluster in the electron transport chain show magnetic couplings distinct from anaerobic [NiFe] hydrogenases (23). One hypothesis states that these couplings could possibly be related to the MBH's oxygen tolerance. This area is still not completely clear, and is the subject of current research. Whatever the reason, oxygen tolerance would be a positive trait in a preparing a photocatalytic module, and it is utilized here.

### **Recent and Ongoing Experiments in Hydrogenase Artificial Catalysis**

The [Fe-Fe] hydrogenase of *Clostridium acetobutylicum* has recently been modified via this same molecular wire method of substituting an exogenous sulfide ligand into the distal [4Fe-4S] of the electron-transport chain (Fig. 4). On coupling to the F<sub>B</sub> cluster of Psac

on PSI via a 1,6-hexanedithiol wire, this module has shown H<sub>2</sub>-producing capacity. Optimization of solution and molecular wire for H<sub>2</sub> production remains to be done. (Golbeck abstract, data unpublished).

The thiol-molecular wiring of an [NiFe] hydrogenase has not yet been attempted. However, previous research with molecular wiring gives reason to believe that this technology may be possible. As mentioned above, the MBH's reaction is reversible and bidirectional given the right conditions. The redox potentials of the clusters in MBH are theoretically compatible to use with PSI, which has a lower potential in the distal cluster (F<sub>B</sub>, in PsaC):  $E'^{\circ}_{FB} = -580\text{mV}$  (17). In addition, the distal [4Fe-4S] cluster of HoxK is located near the surface of the protein, where it normally acts to donate electrons HoxZ. This location is suspected to allow easier coordination to a molecular wire.

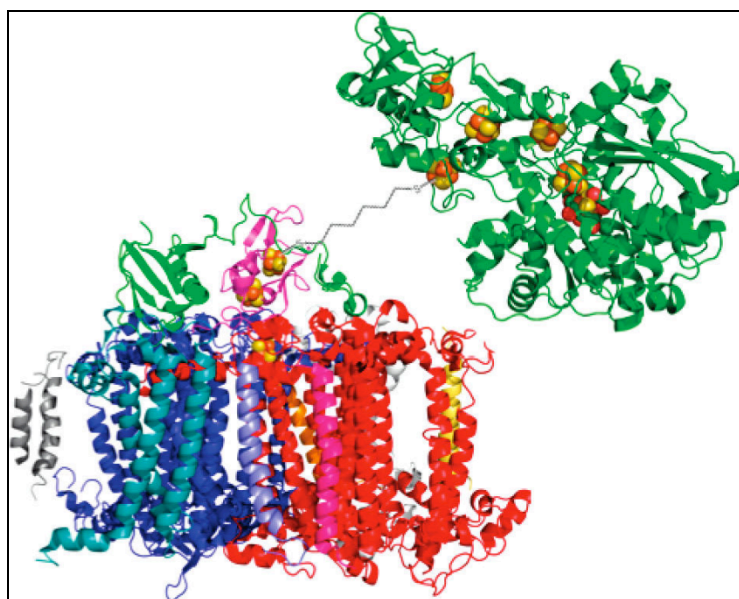


**Fig. 4. Molecular Wiring of PSI to an [FeFe] hydrogenase via 1,6-hexanedithiol.** Similar to that envisioned here with an oxygen-tolerant [NiFe] hydrogenase. From Lubner et. al. 2009. (17).



## Expression and Characterization of a HoxK Variant

In this study, a histidine ligand to the distal [4Fe-4S] cluster in HoxK has been converted to a glycine to open up the coordination site to exogenous ligand (H187→G). The recombinant HoxK was overexpressed in and purified from *E. coli* without the large subunit. After Fe-S reconstitution with stoichiometric ferrous ammonium sulfate and sodium sulfide, low-temperature X-band EPR spectroscopy was performed. The spectra confirm the formation of Fe-S clusters in the recombinant protein, though coupling with the large subunit and PSI remains to be achieved.

In addition to HoxK, the PsaC C14G/C34S variant and PSI of the marine cyanobacterium *Synechococcus* sp. PCC 7002 have been purified for use in the molecular wire.

This research demonstrates an important first step in the molecular wiring of the *R. eutropha* MBH enzyme to build a directly-coupled, atmospheric oxygen-tolerant hydrogen synthesizing module. The major aim of the study presently is confirming the presence of the rebuilt Fe-S clusters involved in electron transport and catalysis. Also, EPR has not been reported on the small subunit alone before. Thus, this research may not only be significant in the construction of a hydrogen-producing catalyst, but possibly also in describing the structure, function and O<sub>2</sub> tolerance of the MBH.

## METHODS:

### **Cloning of *hoxK* mutant gene into *Escherichia coli***

A mutant *hoxK* (H187G) gene containing a *Strep*-tag was cloned into *E. coli* plasmid pASK-IBA3 by restriction at *NcoI* and *BglII* (sites 138 and 152, respectively) by collaborators O. Lenz, et. al. (see Fig. 5). Codons for the C-terminal 43 residues, putatively involved in membrane association and containing the twin arginine TAT signal, were removed (1). Due to poor rates of expression and difficult purification under the tetA promoter in pASK-IBA3, collaborator T. Schubert cloned the fragment into the multiple cloning site of a pET-15b plasmid by restriction at *NcoI* and *HindIII* (bp 177), thus incorporating a *Strep*-tag and putting the gene under the control of a T7 promoter. The pET15b His-tag was not included due to stop codons in the transferred gene. (See Appendix A for WT and mutant DNA and protein sequences).

Electrically competent Rosetta strain *E. coli* cells (from Novagen, containing the pRARE plasmid, encoding for rare amino acids and chloramphenicol resistance) were transformed with the plasmid pET-15b containing mutant *hoxK* and selected by plating on LB agarose with 100 µg/mL ampicillin and 25 µg/mL chloramphenicol.

### **Cell Culture and HoxK Expression**

Cells were grown in 6 1-L flasks of Luria broth (LB) media at 37° C in an incubator with shaking at 200 rpm. (See Appendix B for media and solutions). Cells harboring mutant *hoxK* plasmids and pRARE were selected for by 100 mg/L ampicillin and 25 mg/L chloramphenicol. To scale-up, colonies from plates were first grown in 100 mL cultures

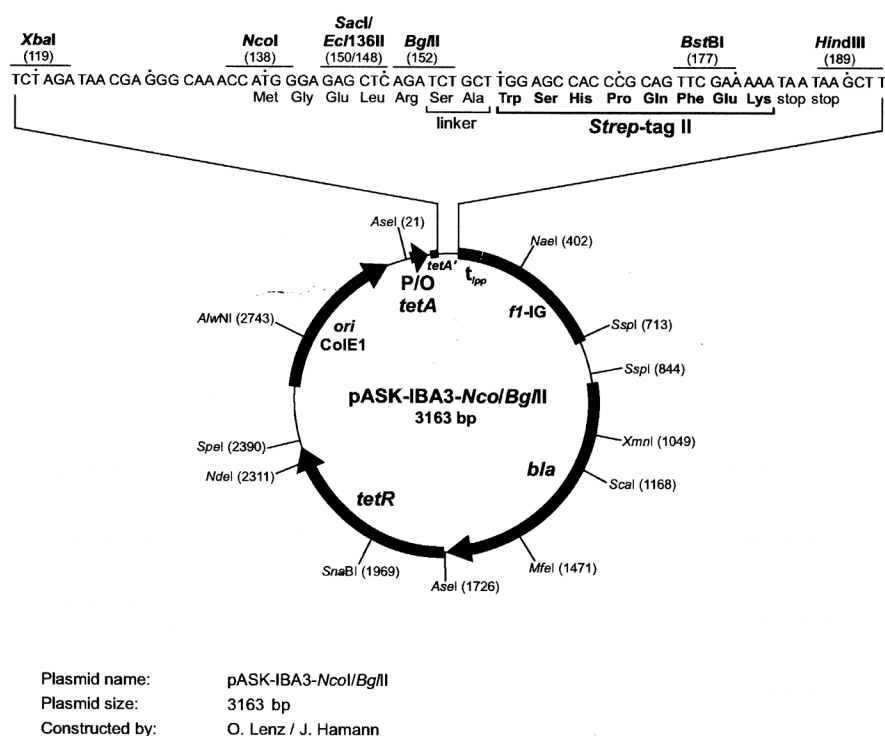


**Fig. 5. The pASK-IBA3 plasmid.** H187G *hoxK* without the C-terminal sequence was first cloned into this tet<sup>R</sup> plasmid by NcoI/BglII restriction. It was removed by NcoI/HindIII restriction to include the *Strep*-tag and cloned into the multiple cloning site of commercially available pET-15b plasmid (Appendix A). From O. Lenz.

until an optical density (O.D.) of at least 0.6 at 600 nm (16-18 h). One-L cultures were inoculated with 10 mL of these cells, grown to an O.D.<sub>600 nm</sub> of 0.6, induced, and incubated for 6-10 hr. Cell growth over time was monitored by O.D. at 600 nm and by SDS-PAGE of lysed whole cells.

### Purification of HoxK H187G

After growth, all purification steps were performed at 4° C. Whole cell pellets were obtained by centrifugation at 11300 x *g* for 10 min. Cell pellets were washed by resuspension and rehomogenization in 50 mM TRIS-HCl, pH 8.3, 20 mM NaCl (Buffer 1) twice, centrifuging 7740 x *g* for 10 min after each resuspension. A total volume of about 80 mL was used for each wash. Cells were resuspended in about 75 mL Buffer 1 with 4 mM 2-mercaptoethanol. Cells were passed through a French pressure cell press twice at 1100

psi. Lysed cells were centrifuged at 3020  $\times g$  for 30 min. Pellets containing inclusion bodies were collected and resuspended/rehomogenized in 40 mL Buffer 1 with 4 mM 2-mercaptoethanol and centrifuged again under the same conditions.

Numerous methods were attempted to solubilize the MBH small subunit variant from the pellets obtained after French press. Among these, solubilization in Buffer A (100 mM Tris-HCl pH 8.0, 150 mM NaCl) with 2% Triton X-114, 1 mM EDTA was attempted. From here on, “non-solubilized” refers to samples of pellets resuspended in 50 mM Tris-HCl pH 8.3/20mM NaCl/4mM 2-mercaptoethanol at this point with no further solubilization. Note: All steps containing Triton X-114 must be kept below the cloud point (20° C) to avoid phase separation. (See Appendix C for further purification techniques performed.)

Protein concentrations in non-solubilized samples were determined by the Bradford method with a bovine serum albumin (BSA) standard curve. For samples containing Triton X-114, a Pierce 660 protein assay was used with BSA standards. Purification steps were recorded by SDS-PAGE 12% run at 30 mA.

### **Western Blot**

Western blot analysis was performed on samples from purification of HoxK variant. Proteins were transferred to nitrocellulose membranes using a Bio-Rad Trans-Blot SD semi-dry transfer cell. Gels were transferred for 30 min at 15 V, with transfer buffer (48 mM Tris/39 mM glycine/20% methanol). Membranes were blocked with 3% BSA/0.5% Tween-20 in PBS buffer (4 mM  $\text{KH}_2\text{PO}_4$ , 16 mM  $\text{Na}_2\text{HPO}_4$ , 115 mM NaCl, pH 7.4). Strep-tagged H187G was detected by Strep-Tactin horseradish peroxidase conjugate according manufacturer’s directions except that a 1:12500 antibody:solution ratio was used. Blots

were developed on film with an Enhanced Chemiluminescence (ECL) kit luminol-based reaction.

### **Iron-Sulfur Cluster Reconstitution**

Electron-transport chain iron-sulfur clusters were reconstituted in HoxK H187G by addition of ferrous iron and sulfide ion in an anaerobic chamber. All steps in this section were carried out anaerobically. To a solution of 50 mM Tris-HCl pH 8.3/4% 2-mercaptoethanol/100  $\mu$ M unsolubilized HoxK H187G (calculated from total protein concentration), 60 mM  $\text{Fe}(\text{NH}_4)_2(\text{SO}_4)_2$ /50 mM Tris-HCl pH 8.3 was added to a final  $\text{Fe}^{2+}$  concentration of 800  $\mu$ M. Then 60 mM  $\text{Na}_2\text{S}$ /50 mM Tris-HCl pH 8.3 was added to a final concentration of 800  $\mu$ M as well. Samples were incubated at 4° C for 12 h. These reconstituted samples were concentrated and washed with buffer (50 mM Tris-HCl pH 8.3) in Amicon 50 mL and 10 mL ultrafiltration systems, MWCO 30 kDa, down to 3 mL. Concentrated samples were passed through PD10 desalting columns and concentrated to 2 mL.

PsaC C14G/C34S reconstitution was performed in the same way, except with 800  $\mu$ M  $\text{Fe}^{2+}/\text{S}^{2-}$ , as it contains two [4Fe-4S] clusters. Iron-sulfur reconstitution of solubilized HoxK H187G was performed in the same way but with a protein concentration of 10  $\mu$ M and excess (50  $\mu$ M)  $\text{Fe}^{2+}/\text{S}^{2-}$ . Desalting was achieved by centrifugation and resuspension in buffer to 50  $\mu$ M.

Two 1-mL aliquots of non-solubilized reconstituted protein were microfuged for 5 min at 500 rpm. The supernatant and pellet, resuspended in 1 mL 50 mM Tris-HCl pH 8.3, were analyzed on SDS-PAGE 12% gels.

## PsaC C14G/C34S Expression and Purification

The 8.6 kDa PsaC subunit (C14G/C34S variant) of the *Synechococcus* PCC 7002 PSI reaction center was cloned into *E. coli* strain BL21 in a pET-3d plasmid, as described previously (30). Cells were grown at 37° C in 6 1-L cultures of LB media with 100 mg/L ampicillin. At O.D.<sub>600nm</sub> (about 3 h), cultures were induced with 0.12 g/L IPTG and grown for 10 h.

All purification steps were performed at 4° C. Whole cell pellets were obtained by centrifugation at 11300 x *g* for 10 min. Cells were resuspended and rehomogenized twice, with centrifugation at 7740 x *g* for 10 min after each. Cells were resuspended in Buffer 1 with 4 mM 2-mercaptoethanol and lysed twice by French pressure cell at 1100 psi. Lysed cells were centrifuged at 3020 x *g* for 30 min. Pellets containing inclusion bodies were collected and resuspended/rehomogenized in 40 mL Buffer 1 with 4 mM 2-mercaptoethanol and centrifuged again under the same conditions. Pelleted PsaC in inclusion bodies were solubilized by stirring for 12 h in 5-10 ml 50 mM Tris pH 8.3, 40 mM 2-mercaptoethanol, 9 M urea. The supernatant after centrifugation at 27200 x *g* for 30 min was run on a G75 gel filtration column (bed volume 200 ml). Fractions containing pure PsaC variant were concentrated on a 3 kDa MWCO amicon concentrator at 60 psi.

PsaC variant reconstitution was carried out in the same manner as for HoxK variant, except that 800 μM concentrations were used for both Fe<sup>2+</sup> and S<sup>2-</sup> (as opposed to those used for HoxK), as PsaC contains only two [4Fe4S] clusters (F<sub>A</sub> and F<sub>B</sub>).

### ***Synechococcus* PCC 7002 PSI Growth and Purification**

*Synechococcus* PCC 7002 cyanobacterial cultures were grown in 10-L carboys of A1 media/50 mg/L gentamicin, with constant white light as done before (11). Cultures were grown at 25° C for 2 weeks.

All purification steps were carried out at 4° C. Cell pellets were obtained by centrifugation at 11300  $\times g$  for 10 min, cells were resuspended/homogenized in 100 ml 50 mM Tris-HCl pH 8, and centrifuged/resuspended again. Cells were lysed three times by French pressure cell at 1100 psi. Supernatant after centrifugation at 7740  $\times g$  for 10 min was decanted and centrifuged at 20000  $\times g$ . Now the pellets, containing the thylakoid membranes, were resuspended to a chlorophyll concentration of 10 mg/ml. Membranes were solubilized in 1% dodecyl maltoside (DM)/ 50mM Tris pH 8 for 2 h and ultra-centrifuged at 48000  $\times g$  for 20 min. Supernatant was loaded onto 32-ml 5-20% sucrose gradients (50 mM Tris, 0.05% DM) and ultra-centrifuged in a swinging bucket rotor at 48000  $\times g$  for 16 h. The lower dark green bands, containing PSI trimers, were removed, concentrated, and run on the same sucrose gradients again with no DM. Pellets containing pure PSI were dissolved in 2 ml 50 mM Tris pH 8, 0.05% DM, 15% glycerol and stored at -80° C.

Chlorophyll concentration was determined spectroscopically in 1:50 sample:methanol.

### **Electron Paramagnetic Resonance Spectroscopy**

X-band EPR was run in a Bruker ECS 106 electron spin resonance spectrometer. Reduced spectra were taken at T= 15 K, 9.487 GHz microwave frequency. Two “narrow scans” of the chemically reduced H187G sample, from 3000-4000 G (Gauss, 1 Gauss =

0.0001 Tesla), were run: one at 100 mW microwave power and one at 126 mW. A third “wide scan” spectrum was taken of the chemically reduced sample at 100mW power, from 25 to 4975 G. Narrow and wide scans of oxidized solubilized H187G (50  $\mu$ M protein) were run at T = 19K, 9.484 GHz microwave frequency. Baseline spectra of 50 mM Tris buffer were also run.

For reduced EPR samples, 0.18 mL sample was combined in the anaerobic chamber with 0.02 mL anaerobic 1 M glycine pH 10, 60 mg/mL sodium dithionite. “Oxidized” samples were run as purified after removal of excess 2-mercaptoethanol. Samples were injected into EPR tubes, removed from the anaerobic chamber and immediately frozen in ethanol in liquid nitrogen.



## RESULTS:

**HoxK Purification**

As seen in Fig. 6, the HoxK variant shows up in the SDS-PAGE at the expected ~35 kDa. A significant band just below 35 kDa was also observed. This has been seen before in MBH purification from other sources, and has been attributed to a likely break-down product. Western blot analysis confirmed the presence of *Strep*-tagged HoxK variant at the position just under 35 kDa, pointed out in Fig. 6.

In some preparations, cell lysate solution became very viscous on a second pass through the French Press, possibly due to DNA.

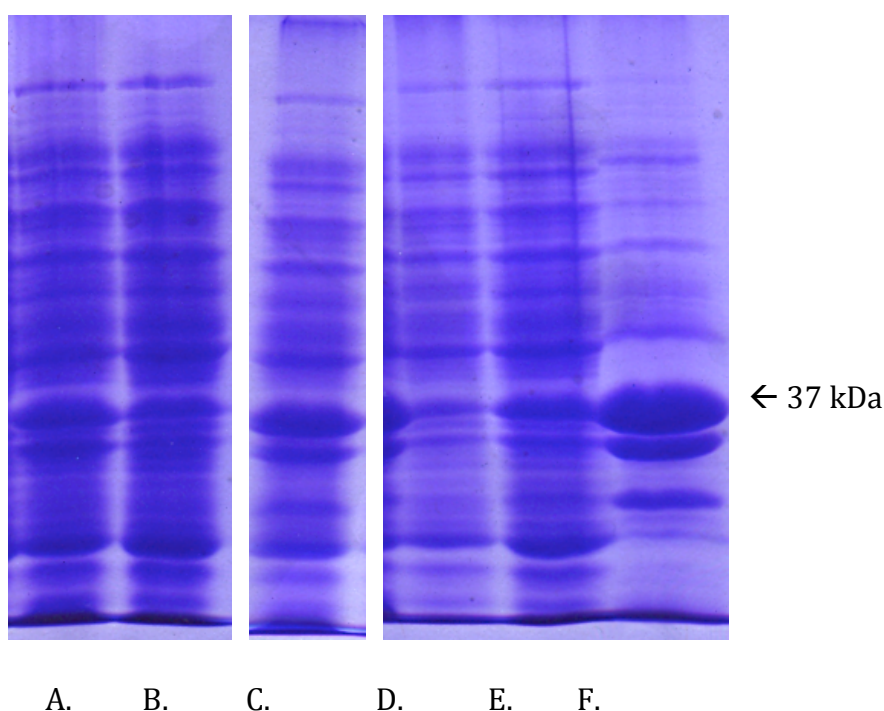


**Fig. 6. Purification of Hoxk variant after French press.** **A.** Insoluble fraction after French Press. **B.** Supernatant after French Press. **C.** Proteins following incubation with 2% Triton X-114/150mM NaCl/50mM Tris-HCl pH 8.0. **D.** Proteins solubilized in supernatant after centrifugation at 7740 x *g*. **E.** Lower, darker pellet after solubilization. **F.** Insoluble pellet fraction, enriched in Hoxk variant. Stained with Coomassie brilliant blue.

T7 promoter was shown to have very leaky expression, with significant expression of HoxK without induction. Western blot confirmed the production of *Strep*-tagged HoxK at 35 kDa in both induced and uninduced cultures.

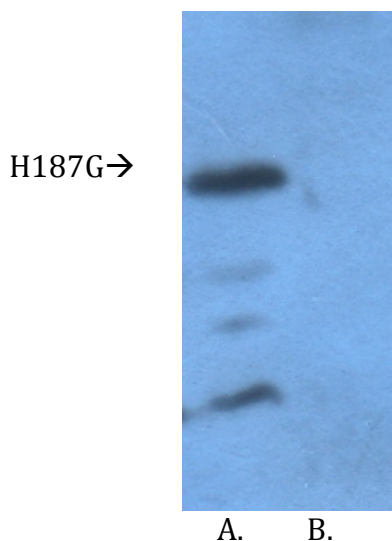


**Fig. 7. Western Blot of hoxK H187G with *Strep*-tag.** **A.** Pelleted fraction after French Press, showing streptavidin binding, presumably to HoxK H187G. **B.** Precision Plus protein standards do not bind streptavidin.

Solubilization of the HoxK variant with Buffer A/2% Triton X-114 proved ineffective in this system. However, it was found that on treatment with Triton X-114, two layers would form in pelleted fractions. The variant was significantly enriched in the upper, white pellet fractions. (See Fig. 6). Appendix C may be consulted for discussion of further attempted purification schemes.

### Iron-Sulfur Cluster Reconstitution

Iron-sulfur cluster formation of HoxK H187G was preliminarily confirmed by color change in solutions (as compared to  $\text{Fe}^{2+}$  and  $\text{S}^{2-}$ -treated reconstitution buffer or 100  $\mu\text{M}$  BSA in reconstitution buffer). As mentioned, insolubility has complicated the purification of MBH dimer proteins in the past. Interestingly, iron-sulfur cluster reconstitution of

unsolubilized HoxK-containing fractions appeared to aid in the solubility of this hoxK variant, either through conformational or solution changes (see Fig. 8 below).

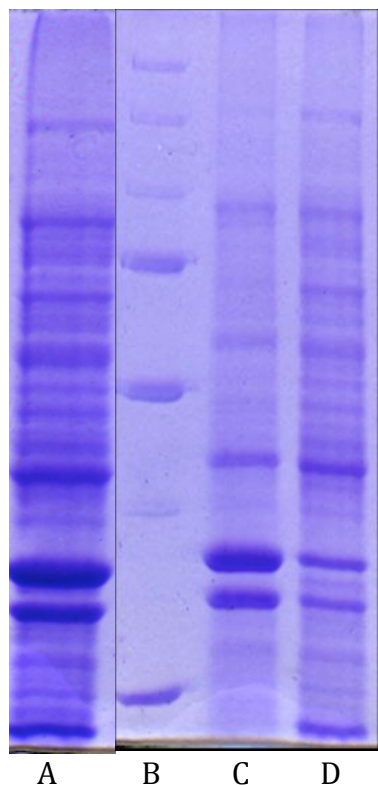


**Fig. 8. Increased solubility of MBH small subunit after Fe-S reconstitution.** **A.)** HoxK variant after reconstitution before centrifugation. **B.)** Precision Plus protein standards. **C.)** Supernatant after centrifugation at  $3020 \times g$  for 5 min. **D.)** Pellet resuspended in 50 mM Tris-HCl pH 8.3. For A, C, and D, 20  $\mu$ l was loaded. 10  $\mu$ l of standards was loaded in B.

### Electron Paramagnetic Resonance

The narrow scan and wide scan spectra of the dithionite-reduced HoxK (Figs. 9 and 10) confirmed the successful reconstitution of iron-sulfur clusters in the unsolubilized HoxK variant. (Narrow scans at both 100 and 126 mW are reported in Fig. 9.) All three spectra showed the same signals, with most signal between 3000 and 3700 G. The spectrum showed a weak but definite signal, due to low protein concentration in the sample. The strong feature at  $g = 2.02$  may mostly be attributed to the background signal. Fig. 11 shows the background signal of this EPR machine with a 50 mM Tris buffer blank.

The strong derivative feature upfield around  $g = 1.93$  in the reduced spectrum is the most significant. Comparison with past spectra on the wild-type MBH subunit from *R. eutropha* may suggest that this broad feature is due to reduced  $[4\text{Fe-4S}]^+$  cluster(s), two of which are present in wild-type HoxK (see Figs. 14C and 15A) (23). There may be some weak coupling of this site to another paramagnetic center, but a stronger spectrum is needed to be sure. It is not possible from this spectrum to determine which cluster this signal would come from, or if both have been introduced into the mutant. There is a consistent set of other features downfield of  $g = 2$  in this spectrum that may suggest spin-spin coupling. The strong background makes it difficult to determine if there is any feature from  $[3\text{Fe-4S}]$  clusters, which would show up around  $g = 2$ . With dithionite at pH 10, however, even if such clusters were present they would presumably be reduced to  $[3\text{Fe-4S}]^0$  and show a very low signal, thus reinforcing the attribution of the  $g = 2.02$  signal to background. (See this trend in Fig 14). Reduced  $[3\text{Fe-4S}]^0$  clusters are paramagnetic but have integer spins, as opposed to the  $s = \frac{1}{2}$  spin of  $[3\text{Fe-4S}]^+$ . Such integer-spin clusters are better detected by an EPR spectrometer with microwave radiation parallel to the magnetic field (as opposed to perpendicular radiation used here) (Golbeck, communication).

The oxidized narrow scan spectra are not conclusive as to whether there is an Fe-S signal. In this spectrum, we were probing for a  $[3\text{Fe-4S}]^+$  medial cluster, as this is the main feature in oxidized MBH dimers, and it is part of HoxK. (Reminder: Ni active site signals would not be seen here because this is the small subunit.) (16). Again, there is a large signal from background near  $g = 2$ .

The  $[3\text{Fe-4S}]^+$  cluster showed a strong signal at  $g = 2.0$  in X-band EPR of MBH dimers (23). This is also similar to the  $[3\text{Fe-4S}]^+$  cluster signal in *Desulfovibrio vulgaris*

Miyazaki F [NiFe] hydrogenase. It is possible that a signal from this cluster is present here, as the background spectrum is somewhat different than the oxidized spectrum. The protein signal must be stronger to determine this.

It should be noted that the spectra in Saggu et. al. (23) used for comparison here are at lower pH (7.0). This may have some effect on the states of the clusters.

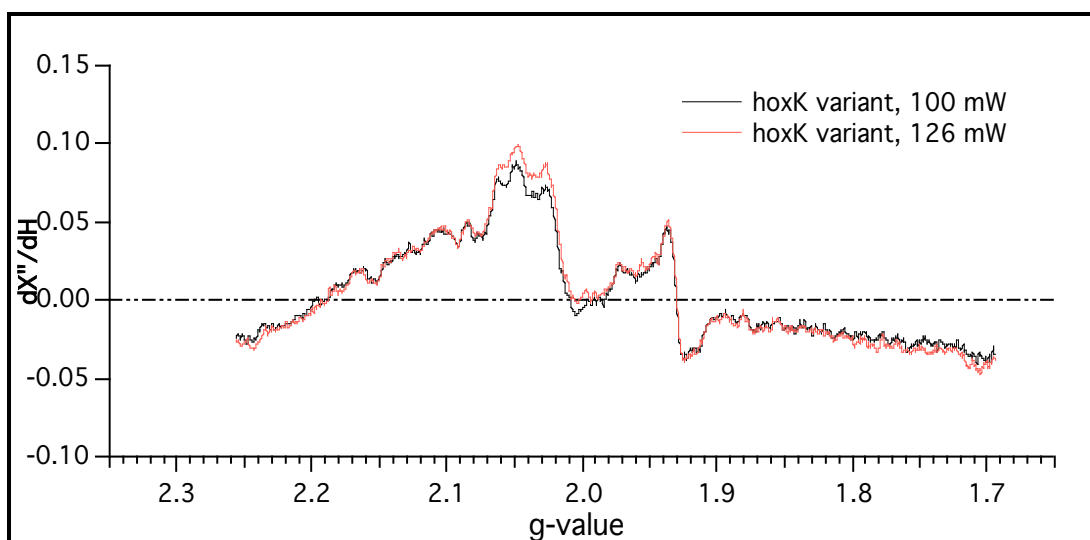


**Fig. 9 X-band (9.487 GHz) EPR of reduced HoxK variant. A (black):** 100 mW microwave power. **B (red):** 126 mW power. Experimental conditions: T= 15 K, pH = 10, B= 3000-4000 G. These spectra are 8 accumulated scans.

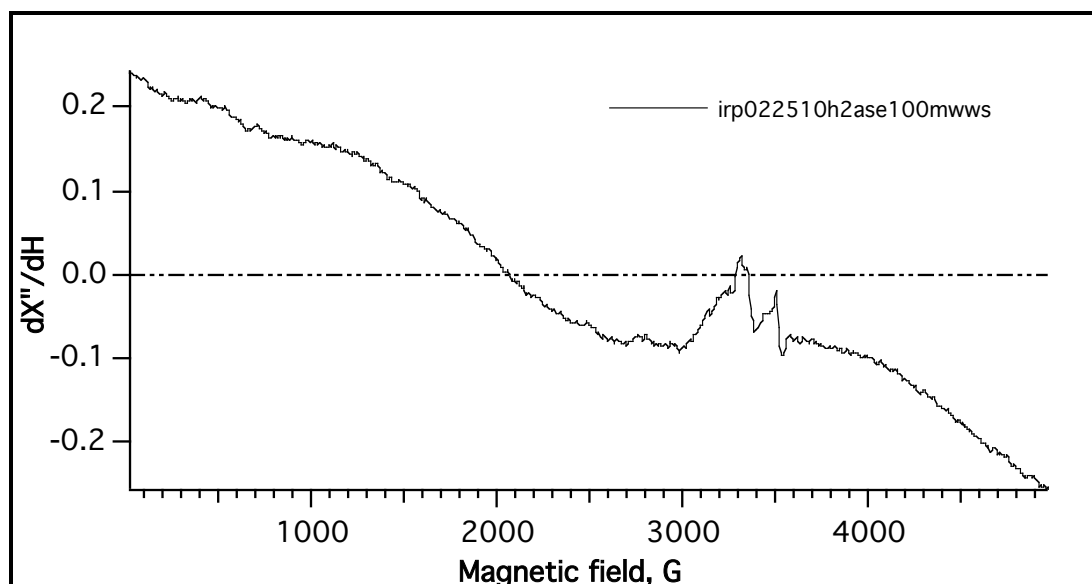


**Fig. 10. X-band (9.487 GHz) EPR of dithionite-reduced HoxK variant. 100 mW microwave. T=15 K. Spectrum is 8 accumulated scans.**

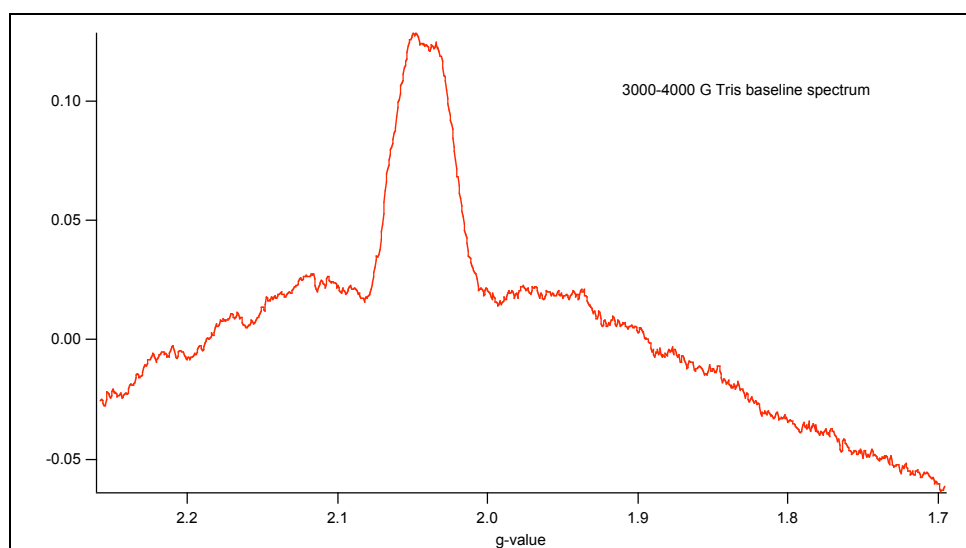


**Fig. 11. X-band EPR 50 mM Tris background spectrum. Note the prominent feature between  $g = 2.0$  and  $g = 2.1$ . Conditions: 20 K, 126 mW.**

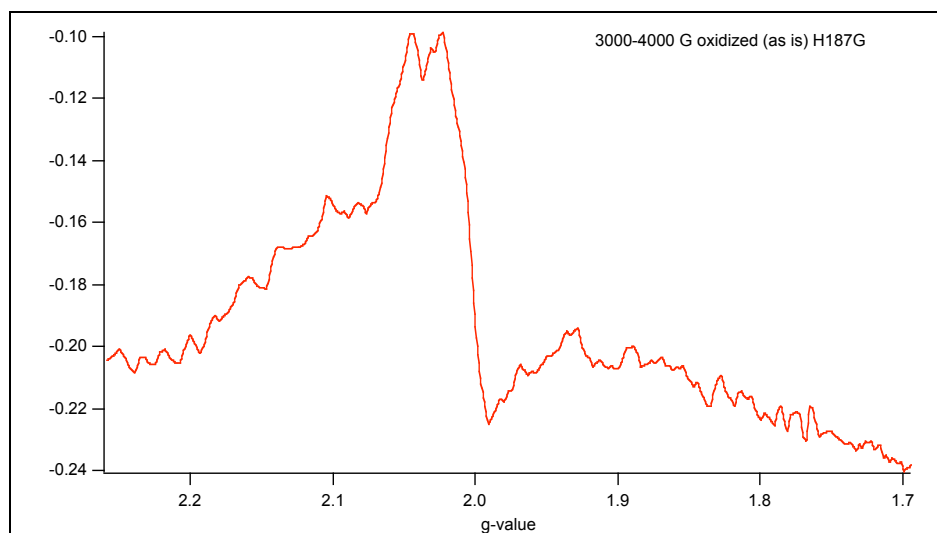


**Fig. 12. Oxidized HoxK H187G. T = 19 K. pH= 8.3. 9.484 GHz microwave frequency. 100 mW. Accumulation of 4 scans.**

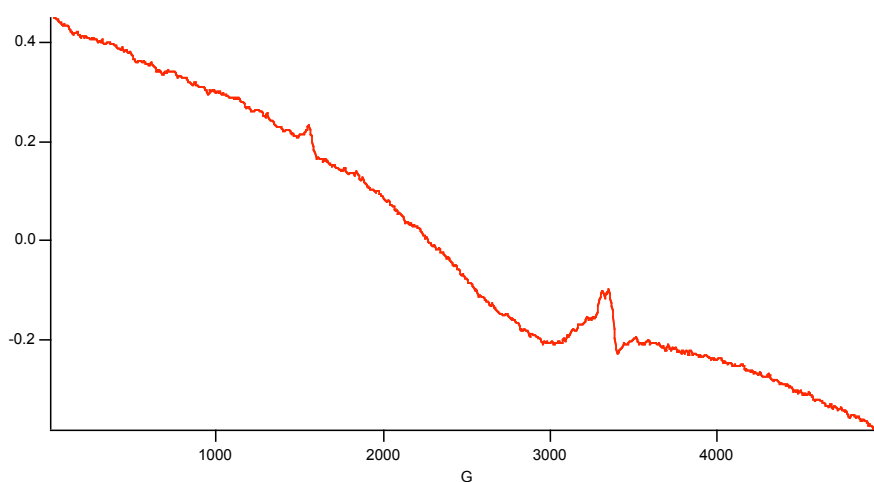


**Fig. 13. Oxidized HoxK H187G wide scan. T = 19 K. pH= 8.3. 9.484 GHz microwave frequency. 100 mW. Accumulation of 4 scans.**

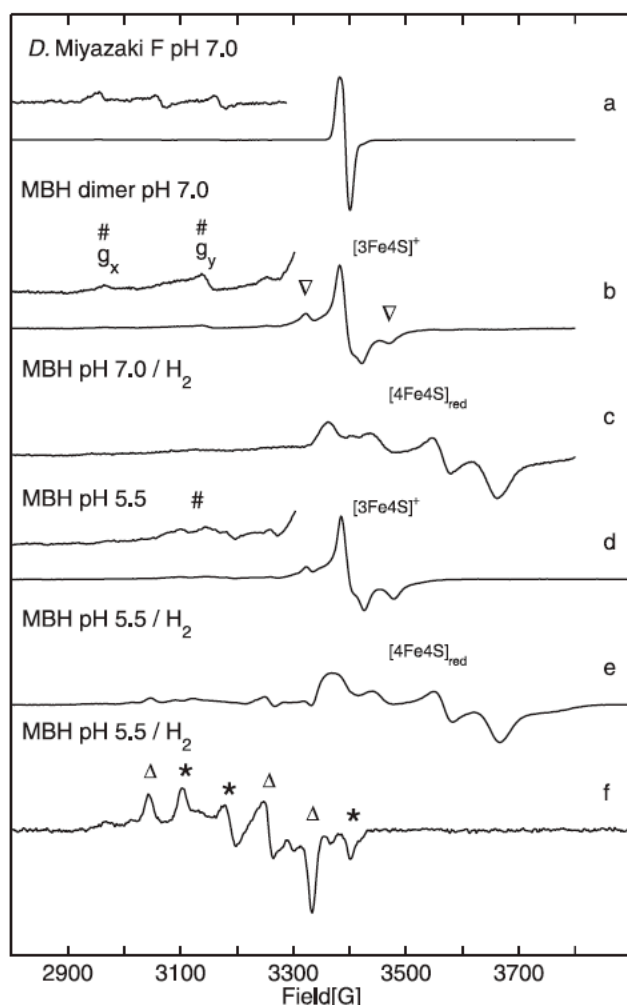


**Fig. 14. “EPR spectra of solubilized MBH dimer showing signals from the [NiFe] and [FeS] centers.”** “The enhanced traces of the spectra show the range of nickel signals with five times increased amplification. Definition of symbols is as follows: #, Nir-B;  $\Delta$ , Nia-L; \*, Nia-C; f, split signal from  $[3Fe4S]_-$ . Trace a, oxidized (as isolated) *D. vulgaris* Miyazaki F hydrogenase. The enhanced trace shows signals from superimposed  $g_x$  and  $g_y$  components of Niu-A and Nir-B. Trace b, oxidized (as isolated) *R. eutropha* MBH protein solution at pH 7.0 saturated with air, showing signals of the  $[3Fe4S]_-$  cluster and Nir-B state. Trace c, H<sub>2</sub>-reduced (1 bar H<sub>2</sub>) *R. eutropha* MBH sample (pH 7.0) displaying signals from reduced  $[4Fe4S]$  centers. Trace d, oxidized (as isolated), and trace e, H<sub>2</sub>-reduced (1 bar H<sub>2</sub>) *R. eutropha* MBH samples at pH 5.5. f, H<sub>2</sub>-reduced (1 bar H<sub>2</sub>) *R. eutropha* MBH at T<sub>80</sub> K, showing a superposition of signals from the Nia-C and Nia-L states. Experimental conditions for spectra (traces a–e) T<sub>20</sub> K, (f) T<sub>80</sub> K; 1 milliwatt microwave power; microwave frequency 9.56 GHz; 1 mT modulation amplitude, 12.5 kHz modulation frequency.” Taken from Saggu, et. al. (23).

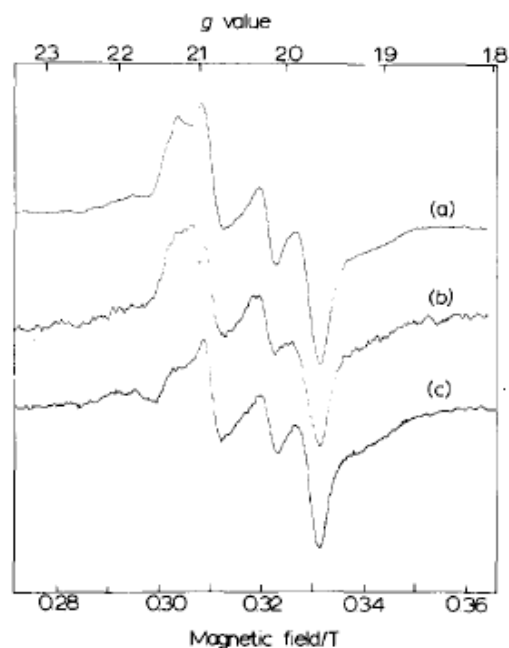


**Fig. 15.** (a) and (b) show low-temperature X-band EPR spectra of reduced *Ralstonia* MBH, showing similarities to the HoxK variant, presumably from reduced, coupled  $[4Fe4S]^+$  cluster(s). Taken from Schneider et. al. (24). Note: g-values are offset in this source.



## DISCUSSION:

### **Analysis of New HoxK H187G Purification Scheme**

French Press and separation by centrifugation in Buffer 1 resulted in insufficient removal of protein impurities. HoxK remained insoluble, as shown in past work, despite removal of the C-terminal sequence involved membrane localization and association. However, the HoxK variant was overproduced enough in *E. coli* with this genetic construct that it constituted the majority of the insoluble fractions. Indeed, it was enough to warrant sufficiently strong signal for EPR studies after Fe-S reconstitution.

Resuspension in Buffer A/Triton X-114 2% solutions improved HoxK purity in insoluble fractions by solubilization of other proteins, which were then separated by centrifugation. It was also found that the top, softer, white layer of multi-layer pellets after Buffer A/2% Triton X-114 solubilization was enriched in HoxK, while the lower pellet and supernatant contained very little. After reconstitution, an increase in the solubility of the HoxK variant was apparent, although lower centrifugation levels were used.

### **EPR Spectral Analysis**

The X-band EPR spectra of the newly purified, reconstituted HoxK variant suggest the presence of reconstituted Fe-S clusters, specifically  $[4\text{Fe-4S}]^+$  cluster(s) under reducing conditions. However, better spectra are needed provide better evidence of the states of these clusters, and whether a true holo-subunit has been achieved is still not clear. I will attempt to obtain stronger, clearer signals by increasing protein concentration and purity, and running more scans for each spectrum. Optimum reconstitution conditions for HoxK variant also remain to be determined. Chemical assays for iron and sulfur content in the reconstituted proteins should aid in determining what conditions best foster Fe-S cluster

formation in this variant. The midpoint potentials of reconstituted variant clusters, which are important to electron transfer in catalysis and may be altered by the mutation, could be determined by titration and EPR studies. In addition, the spectra of HoxK at lower pH and under more oxidizing conditions (as done with the MBH dimer by 23) may also provide insight into the structure and electronic interactions of the recombinant electron transport chain. Mossbauer spectroscopy may also be useful in this case, as Fe atoms are in each of the clusters. In a similar case, alteration of ligands to the  $F_B$  cluster of PsaC showed considerable spectroscopic alteration (30, 17). Catalytic activity may be difficult to obtain, but the reconstitution of Fe-S clusters is essential.

### **Future Directions**

The significance of the presence of Fe-S clusters is that further incubation with “molecular wires” may allow successful displacement of 2-mercaptoethanol at the distal [4Fe4S] cluster. Further EPR spectra will hopefully identify the electron transfer sites in hoxk H187G. PsaC C14G/C34S variant, as purified from *E. coli*, has already been demonstrated to be conducive to the spontaneous association with PSI (also purified here) and molecular wiring.

Based on this data and past work, a PSI-PsaC-HoxK molecular wire could theoretically be constructed (17, 11, 10). Hence, further optimization of purification of the HoxK variant is warranted. The next step in this research would be toward such a construct. Spectroscopic studies with such a construct would need to be performed to determine if electrons could successfully be transferred to the Fe-S clusters of HoxK via the molecular wire from Psac-PSI.

The last protein component of the full half-cell module hypothesized in this study is the HoxG large subunit. HoxG has been purified from *R. eutropha* without the small subunit (29). Interestingly, the full MBH operon, with both enzyme and maturation protein genes (e.g all Hox genes), has been cloned into a megaplasmid and expressed in MBH-free *R. eutropha* and in *Pseudomonas stutzeri*, conferring hydrogen oxidizing ability (15). Expression of this operon has not yet been reported in an *E. coli* system. For these proof-of-concept experiments, HoxG will most likely be expressed by itself in *E. coli*, with subsequent active site metal reconstitution. This will require a novel genetic construct for expression and a Ni-Fe reconstitution procedure, which has not yet been performed.

The possibility of H<sub>2</sub>-production with this module seems reasonable. However, the true efficacy and oxygen tolerance of this module remain to be investigated. Note that the efficiency of PSI is unquestioned. PSI is also robust: all components are stable and withstand moderate heat and light levels (17).

The catalytic rate and cost efficiency of PSI-hydrogenase modules remains to be optimized, as do those all photocatalytic hydrogen production systems. Experimentation with different molecular wires will no doubt play a role. This engineering will ultimately determine the usefulness of hydrogenase conjugates in energy production. As seen in Table 2, the highest rate of PSI-coupled hydrogen production is via molecular wire attachment to platinum nanoparticles, at rates of 312  $\mu\text{mol}$  of H<sub>2</sub> per mg chlorophyll per hour. This is equivalent to 90 Joules per hour or 0.025 Watts per mg chlorophyll, assuming all of the 143 kJ/g available in the combustion of H<sub>2</sub> is harnessed. The rate for PSI-[FeFe] hydrogenase is about two orders of magnitude lower (3.9  $\mu\text{mol}/\text{mg Chl}/\text{h}$ ). Though this

may be low, it is a powerful proof of concept, and the altering of molecular wires and other variables may hopefully improve this rate dramatically.

	<b>Rate of H<sub>2</sub> production [<math>\mu\text{mol H}_2</math> (mg of Chl)<sup>-1</sup> h<sup>-1</sup>]</b>
<b>Metal systems</b>	
platinized PS I	0.025
PC-cross-linked platinized PS I	0.080
osmium-coated chloroplasts	0.113
PS I-molecular wire-Au nanoparticle	3.4
PS I-molecular wire-Pt nanoparticle	9.6
PS I-molecular wire-Pt nanoparticle with Cytochrome <i>c</i>	49.3
PS I-molecular wire-Pt nanoparticle (optimized)	312
<b>Enzyme systems</b>	
PS I-H <sub>2</sub> ase-soluble electron donors	0.58
PS I-molecular wire-H <sub>2</sub> ase	3.9

**Table 2. Comparative Rates of Light-Induced Production of Hydrogen from Inorganic and Proteinaceous Catalytic Systems. Adapted from Lubner, et. al. 2009. (17).**

The direct coupling of PSI to the membrane-bound [NiFe] hydrogenase of *R. eutropha* shows an interesting example of utilizing solar energy for the synthesis of H<sub>2</sub>. The direct coupling via a molecular wire has been shown to greatly increase reaction velocity by eliminating rate-limiting diffusion chemistry, as seen in Table 2. The MBH-PSI module considered here would be expected to be in this range, bhe major importance of this hydrogenase is its high oxygen-tolerance compared to other hydrogenase classes. Another important consideration is that gold and platinum catalysts, due to the high value and low abundance of these metals, may be economically prohibitive compared to hydrogenases.

Even if this specific PSI-MBH bioconjugate does not prove economically successful, this project may also confer information about the chemistry and structure of the [NiFe] active site, the protein's means of O<sub>2</sub>-tolerance, and the efficiency of molecular wiring, all of

which may be applied to future synthetic bioconjugates.

#### ACKNOWLEDGEMENTS:

I would like to thank Cara Lubner, Steve Romberger, and Dr. John Golbeck for personally teaching and assisting me during my 3 years working in the Golbeck lab. I would also like to thank Paul and Mildred Berg and Charles and Vickie Grier, who supported me in my research through the Berg Fund and Grier Fund scholarships for summer undergraduate research in 2008. Additionally, I would like to thank William and Joan Schreyer and all donors to the Schreyer Honors College, whose generosity has made countless students able to take advantage of honors research at Penn State.

## REFERENCES:

- 1) **Bernhard M., B. Friedrich, and R. A. Siddiqui.** 2000. *Ralstonia eutropha* TF93 Is Blocked in Tat-Mediated Protein Export. J. Bacteriol. **182**: 581–588.
- 2) **Bernhard, M., B. Benell, A. Hochkoeppler, D. Zannoni and B. Friedrich.** 1997. Functional and structural role of the cytochrome *b* subunit of the membrane-bound hydrogenase complex of *Alcaligenes eutrophus* H16. Eur. J. Biochem. **248**: 179-186.
- 3) **Cracknell, J. A., A. F. Wait, O. Lenz, B. Friedrich, and F. A. Armstrong.** 2009. A kinetic and thermodynamic understanding of O<sub>2</sub> tolerance in [NiFe]-hydrogenases. PNAS **106**: 20681–20686.
- 4) **Cramm, R.** 2009. Genomic View of Energy Metabolism in *Ralstonia eutropha* H16. J Mol Microbiol Biotechnol. **16**: 38–52
- 5) **Dementin,S., V. Belle, P. Bertrand, B. Guigliarelli, G. Adryanczyk-Perrier, A. L. De Lacey, V. M. Fernandez, M. Rousset, and C. Léger.** 2006. Changing the Ligation of the Distal [4Fe4S] Cluster in NiFe Hydrogenase Impairs Inter- and Intramolecular Electron Transfers. J. Am. Chem. Soc. **128**: 5209-5218.
- 6) **Evans B. R., H. M. O'Neill, S. A. Hutchens, B. D. Bruce and E. Greenbaum.** 2004. Enhanced Photocatalytic Hydrogen Evolution by Covalent Attachment of Plastocyanin to Photosystem I. Nano Letters **4**: 1815–1819
- 7) **Fernandez, V. M., E. C. Hatchikiana and R. Cammack.** 1985. Properties and reactivation of two different deactivated forms of *Desulfovibrio gigas* hydrogenase Biochim. Biophys. Acta. **832**: 69-79.

- 8) **Golbeck J. H.** 2010. Biohybrid Systems in Solar Biofuel Production. [Seminar abstract]. <http://bioenergy.asu.edu/cb&p/abstracts/Golbeck-abstract.html>
- 9) **Golbeck, J. H.** 2003. Photosystem I. in Bioenergetics volume of Biophysics Textbook On Line, published by the American Biophysical Society  
<http://www.biophysics.org/btol/>.
- 10) **Golbeck, J. H. and D. A. Bryant.** A Hybrid Biological-Organic Photochemical Half-Cell for Generating Dihydrogen.  
[http://www.hydrogen.energy.gov/pdfs/review08/bes\\_14\\_golbeck-bryant.pdf](http://www.hydrogen.energy.gov/pdfs/review08/bes_14_golbeck-bryant.pdf)
- 11) **Grimme, R. A., C. E. Lubner, D. A. Bryant, and J. H. Golbeck.** 2008. Photosystem I/Molecular Wire/Metal Nanoparticle Bioconjugates for the Photocatalytic Production of H<sub>2</sub>. J. Am. Chem. Soc. **130**: 6308–6309.
- 12) **Ihara M., H. Nishihara, K. Yoon, O. Lenz, B. Friedrich, H. Nakamoto, K. Kojima, D. Honma, T. Kamachi, and I. Okura.** 2006. Light-driven Hydrogen Production by a Hybrid Complex of a [NiFe]-Hydrogenase and the Cyanobacterial Photosystem. Photochem. Photobiol. **82**:676-682.
- 13) **Knüttel K, K Schneider, A Erkens, W Plass, A Müller, E Bill, AX Trautwein.** 1994. Redox properties of the metal centres in the membrane-bound hydrogenase from *Alcaligenes eutrophus* CH34. Bull Pol Acad Sci Chem. **42**: 495– 511.
- 14) **Kortluke, C., K. Horstmann, E. Schwartz, M. Rohde, R. Binsack, and B. Friedrich.** 1992. A gene complex coding for the membrane-bound hydrogenase of *Alcaligenes eutrophus* H16. J. Bacteriol. **174**: 6277-6289.



- 15) **Lenz O., A. Gleiche, A. Strack, and B. Friedrich.** 2005. Requirements for Heterologous Production of a Complex Metalloenzyme: the Membrane-Bound [NiFe] Hydrogenase. *J. Bacteriol.* **187**: 6590-6595.
- 16) **Lenz, O., M. Bernhard, T. Buhrke, E. Schwartz, and B. Friedrich.** 2002. The Hydrogen-Sensing Apparatus in *Ralstonia Eutropha*. *J. Mol. Microbiol. Biotechnol.* **4**: 255–262.
- 17) **Lubner C. E., R. Grimme, D. A. Bryant, and J. H. Golbeck.** 2010. Wiring Photosystem I for Direct Solar Hydrogen Production. *Biochemistry* **49**: 404–414.
- 18) **Ludwig M., J. A. Cracknell, K. A. Vincent, F. A. Armstrong, and O. Lenz.** 2009. Oxygen-tolerant H<sub>2</sub> oxidation by membrane-bound [NiFe] hydrogenases of *Ralstonia* species. Coping with low level H<sub>2</sub> in air. *J Biol Chem.* **284**: 465-7.
- 19) **Malkin, R., D. B. Knaff and A. J. Bearden.** 1973. The oxidation-reduction potential of membrane-bound chloroplast plastocyanin and cytochrome *f*. *Biochim. et Biophys. Acta*, 305: 675-678
- 20) **Müller, M.G., C. Slavov , R. Luthra, K. E. Redding, and A. R. Holzwarth.** 2010. Independent initiation of primary electron transfer in the two branches of the photosystem I reaction center. *PNAS* **107**: 4123-4128.
- 21) **Ohnishi, T.** 1998. Iron–sulfur clusters/semiquinones in Complex I. *Biochimica et Biophysica Acta* **1364**.
- 22) **Pohlmann A., W. F. Fricke , F. Reinecke , B. Kusian, H. Liesegang, R. Cramm, T. Eiting, C. Ewering, M. Pötter, E. Schwartz, A. Strittmatter, I. Vo, G. Gottschalk, A. Steinbüchel, B. Friedrich and B. Bowien.** 2006. Genome

sequence of the bioplastic-producing "Knallgas" bacterium *Ralstonia eutropha* H16. Nature Biotech. **24**: 1257 – 1262.

- 23) **Saggu, M., I. Zebger, M. Ludwig, O. Lenz, B. Friedrich, P. Hildebrandt, and F. Lendzian.** 2009. Spectroscopic Insights into the Oxygen-tolerant Membrane-associated [NiFe] Hydrogenase of *Ralstonia eutropha* H16. J. Biol. Chem. **284**:16264–16276.
- 24) **Schneider, K., D. S. Patil and R. Cammack.** 1983. ESR Properties of Membrane-Bound Hydrogenases from Aerobic Hydrogen Bacteria.. Biochim. Biophys. Acta, **748**: 353-361.
- 25) **Tang, H., K. Prasad, R. Sanjinès, P.E. Schmid and F. Lévy.** 1994. Electrical and optical properties of TiO<sub>2</sub> anatase thin films. J. Appl. Phys. **75**: 2042.
- 26) **Terasaki N., N. Yamamoto, T. Hiraga, Y. Yamanoi, T. Yonezawa, H. Nishihara, T. Ohmori, M. Sakai, M. Fujii, A. Tohri, M. Iwai, Y. Inoue, S. Yoneyama, M. Minakata, and I. Enami.** 2009. Plugging a Molecular Wire into Photosystem I: Reconstitution of the Photoelectric Conversion System on a Gold Electrode. Angewandte Chemie Intl. Ed. **48**: 1585-1587.
- 27) **Vassiliev I.R., M.L. Antonkine and J.H. Golbeck.** 2001. Iron–sulfur clusters in type I reaction centers. Biochim. et Biophys. Acta-Bioenergetics. **1507**: 139-60.
- 28) **Vincent, K. A., J. A. Cracknell, J. R. Clark, M. Ludwig, O. Lenz, B. Friedrich and F. A. Armstrong.** Electricity from low-level H<sub>2</sub> in still air – an ultimate test for an oxygen tolerant hydrogenase. Chem. Commun. **48**: 5033–5035.
- 29) **Winter G., T. Buhrke, O. Lenz, A. K. Jones, M. Forger and B. Friedrich.** Ed. by P. Brzezinski. 2005. A model system for [NiFe] hydrogenase maturation

studies: Purification of an active site-containing hydrogenase large subunit without small subunit. FEBS Letters **579**: 4292-4296.

- 30) **Zhao J., P. V. Warren, N. Li, D. A. Bryant, and J. H. Golbeck.** 1990. Reconstitution of electron transport in photosystem I with PsaC and PsaD proteins expressed in *Escherichia coli*. FEBS Lett. **276**: 175-180.
- 31) **Zouni, A., H.T. Witt, J. Kern, P. Fromme, N.Krauss, W. Saenger and P. Orth.** 2001. Crystal structure of photosystem II from *Synechococcus elongatus* at 3.8 Å resolution. Nature **409**: 739-743.

## APPENDIX A: DNA AND PROTEIN SEQUENCES

### *Ralstonia eutropha* H16 – [NiFe] Membrane-bound hydrogenase protein sequence (14):

```

1  MVETFYEVMR RQGISRRSFL KYCSLTATSL GLGPSFLPQI AHAMETKPRT PVLWLHGLEC
61  TCCSESFIRS AHPLAKDVVL SMISLDYDDT LMAAAGHQAE AILEEIMTKY KGNILAVEG
121 NPPLNQDGMS CIIGGRPFIE QLKIVAKDAK AIISWGS CAS WGCVQAAKPN PTQATPVHKV
181 ITDKPIIKVP GCPPIAEVMT GVITYMLTFD RIPELDRQGR PKMFYSQRIH DKCYRRPHFD
241 AGQFVEEWDD ESARKGFCLY KMGCKGPTTY NACSTTRWNE GTSFPIQSGH GCIGCSEDGF
301 WDKGSFYDRL TGISQFGVEA NADKIGGTAS VVVGAAVTAH AAASAIKRAS KKNETSGSEH

```

In this study, the highlighted 43 amino acids (TAT signal sequence) are removed. The red residues are involved in coordinating Fe-S clusters. His 187 (His 230 in the original sequence) is changed to G in this study.

### *Ralstonia eutropha* H16 – [NiFe] Membrane-bound hydrogenase variant protein sequence, with *Strep*-tag:

```

1  METKPRTPVL WLHGLECTCC SESFIRSAHP LAKDVVLSMI SLDYDDTLMA AAGHQAEAIL
61  EEIMTKYKGN YILAVEGNPP LNQDGMSCII GGRPFIEQLK YVAKDAKAI I SWGSCASWGC
121 VQAAKPNPTQ ATPVHKVITD KPIIKVPGCP PIAEVMGTGVI TYMLTFDRIP ELDRQGRPKM
181 FYSQRI GDKC YRRPHFDAGQ FVEEWDDESA RKGFCLYKMG CKGPPTYNAC STTRWNEGTS
241 FPIQSGH GCI GCSEDGFWDK GSFYDRLTGI SQFGVEANAD KIGGTASVVV GAAVTAHAAA
301 SAIKRASKKN ETSGSEH

```

### Wild-type *hoxK* gene, *R. eutropha* (14):

```

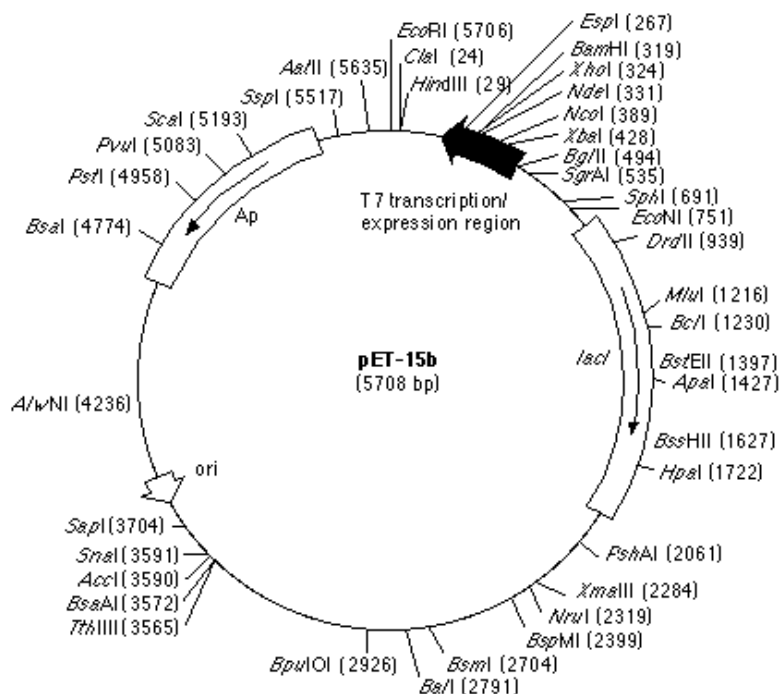
1  atggtcgaaa cattttatga agtcatgcgc aggcagggca tttcgcgcagc aagtttcctg
61  aagtactgtt ccctgacagc cacatcctta ggactgggac cttcctttct gccgcagatc
121 ggcgcacgca tggaaaccaa gccgcgtaca ccagtacttt ggctgcacgg tctcgaatgt
181 acctgttgct cggaatcggt cattcgctcg gcccatccgc tggcaaagga cgtcgtgcta
241 tcgatgatct cactggacta tgacgacaca ctgatggcgg ctgccggcca ccaggccgag
301 gccatcctcg aggagatcat gacgaagtac aagggcaact atattctggc ggtggagggg
361 aatccgccac tcaatcagga tggcatgagc tgcattcatc gtggggcgcc attcattgag
421 cagctcaaat acgtggccaa ggatgccaag gccattatct cctgggggtc ctgcgcattc
481 tgggggatgcg tgcaggcagc caaacctaatt cccactcagg ccacaccggt tcacaaggtg
541 atcaccgaca agccgattat caaggtcccg ggggtgccctc cgattgccga agtgatgacg
601 ggtgtcatta cctacatgct caccttcgat cgtattcccg aactggatcg acagggtcgg
661 ccgaagatgt tctatagcca gcgcatccac gacaaatgct accggcgctc acacttcgat
721 gccggccagt tcgtcgagga atgggacgac gaatcagccc gcaaaggctt ctgcttatac
781 aagatgggct gtaaaggccc gaccacgtac aacgcctgct ccaccacgcg ctggaacgag
841 gggacgagtt tccccattca gtcgggccac ggttgcatg gttgctccga ggatggcttt
901 tgggacaaaag gctcattcta cgatcgtctg accggcatca gccagttcgg cgttgaggcc
961 aacgccgaca agattggcgg aacggcctcc gtcgtggtgg gggcgccgct gacggcgcat
1021 gccgcagcgt ctgcgatcaa gcgtgcgtcg aagaagaacg aaaccagcgg cagtgaacac
1081 taa

```

### Variant *hoxK* gene, with *Strep*-tag:

**pET-15b plasmid map, available from Novagen.** The mutant *hoxK* gene was cloned into the T7 expression region. This map from: ([http://www.merck-chemicals.com/life-science-research/technical-bulletins/c\\_IMOb.s10XkUAAAEj2xsYzMkq](http://www.merck-chemicals.com/life-science-research/technical-bulletins/c_IMOb.s10XkUAAAEj2xsYzMkq))

A



B

BstII T7 promoter lac operator XbaI  
 AGATCTCGATCCGCGAAATTAATACGACTCACTATAGGGGAATTGTGAGCGGATAACAATTCCCTCTAGAAATAATTTGTTTA  
NcoI NdeI  
 AC TTTAAGAAGGAGATATACCATGGGCAGCAGCCATCATCATCATCAGCAGCGGCCGTGGTGCCGCGCGGCAGCCAT  
 MetGlySerSerHisHisHisHisHisSerSerGlyLeuValProArgGlySerHis  
 thrombin  
XhoI BamHI EspI  
 ATGCTCGAGGATCCGGCTGCTAACAAAGCCCGAAAGGAAGCTGAGTTGGCTGCTGCACCGCTGAGCAATAAC TAGCATAACCC  
 MetLeuGluAspProAlaAlaAsnLysAlaArgLysGluAlaGluLeuAlaAlaAlaThrAlaGluGlnEnd  
EcoRV  
 CTTGGGGCCTCTAAACGGGTCTTGAGGGGTTTTTGCTGAAAGGAGGAAC TATACCGGATATC

**APPENDIX B. SOLUTIONS, MEDIA, AND PROTOCOLS**

Buffer 1:

50 mM Tris-HCl pH 8.3, 20 mM NaCl

Buffer A: (as in source 29): 100 mM Tris pH 8, 150 mM NaCl, 1 mM EDTA

**Luria Broth Media**

10g/L NaCl

5 g/L Yeast Extract

10 g/L Tryptone

pH to 7.0 with concentrated NaOH or KOH

**A1 Media**

18 g/L NaCl

0.6 g/L KCl

1.0 g/L NaNO<sub>3</sub>

5.0 g/L MgSO<sub>4</sub>

0.05 g/L KH<sub>2</sub>PO<sub>4</sub>

0.266 g/L CaCl<sub>2</sub>

0.03 g/L NaEDTA tetra

10 mL/L Tris 100g/L pH 8.2

3.89 mg/L FeCl<sub>3</sub>.6H<sub>2</sub>O

1 mL 1000x P1 metals

Autoclave, then to 4 µg/L vitamin B12

## APPENDIX C. ADDITIONAL PURIFICATION METHODS

### **Additional Biochemical Treatments of HoxK**

The HoxK subunit has not previously been purified alone. High insolubility has been observed in both the large and small subunits of the MBH when overexpressed, and thus overcoming this in purification was the most time-consuming portion of this project. For EPR spectroscopy, complete protein purity is not of utmost importance, as long as the species of interest is concentrated enough and aberrant paramagnetic species can be eliminated from solution. Even so, numerous methods to increase purity were attempted, as it may be important for further studies.

Preliminarily, urea solubilization was performed at concentrations of 4.5 M to 9 M urea. H187G remained insoluble in pellets after centrifugation tried at various *g*. Gel filtration (G75), anion exchange (DE52), and Strep-tactin Superflow affinity chromatography were attempted on the Buffer 1-washed pellets.

Further methods of increasing solubility were attempted:

- Vary NaCl concentration up to 1.0 M
- More concentrated Tris: up to 100 mM
- Triton x-100 and x-114 and n-dodecyl maltoside detergents, varied temperatures
- Switching to a phosphate buffer
- Lower pH: phosphate buffer at 7.0, with and without 150 mM NaCl, with and without Triton x-114, with both NaCl and Triton
- Vary the centrifugation speed

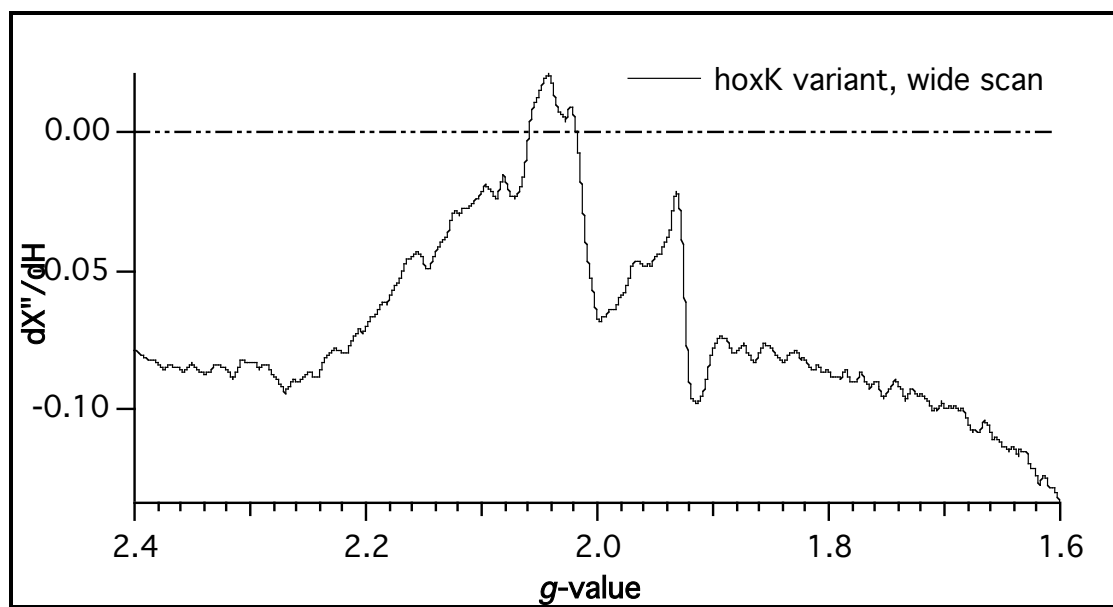
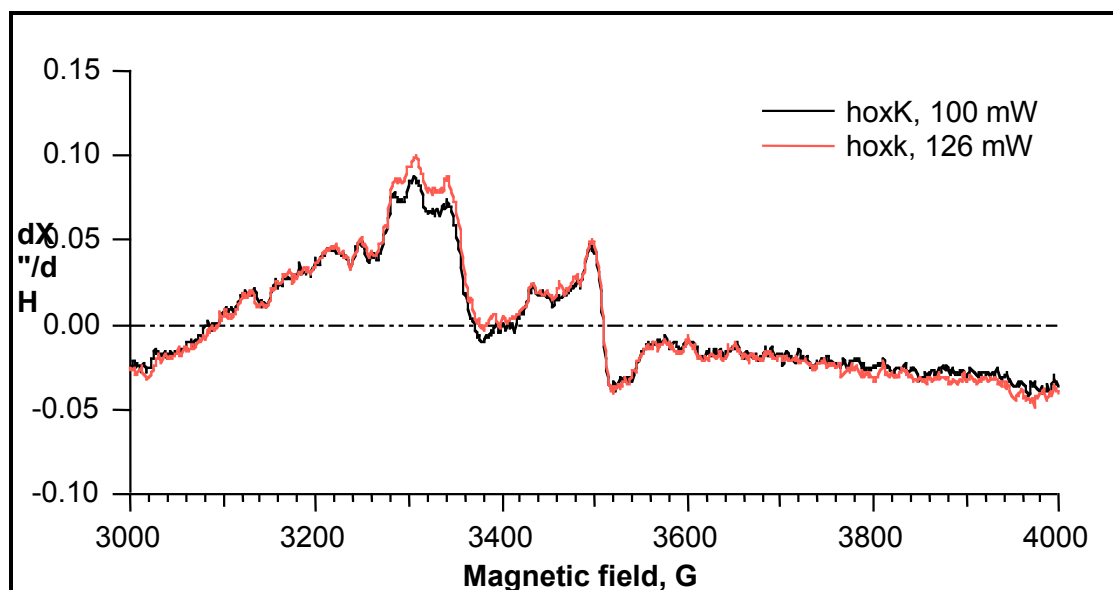
- Eventually, it was found that FeS reconstitution itself aided in solubility, possibly due to conformational changes in the protein, or to increase ionic strength from Fe and S salts.
- Non-solubilized and Buffer A/2% Triton X-114 samples were reconstituted. In addition, an aliquot of non-solubilized sample was treated with Buffer A/2% Triton after reconstitution.



## APPENDIX D: EPR SPECTRA

Note to the reader: EPR spectroscopy is based on the differences in energy between electrons in a magnetic field based on their spin magnetic moments (the Zeeman effect). These differences in energy can be sensed by absorption of microwave frequency photons that carry the same energy as the difference in energy between the electron's two states (aligned with and antiparallel to the magnetic field). Most EPR spectrometers vary the magnetic field, changing the difference in energy between electron spin states, while keeping the microwave frequency the same. Thus, the independent variable is magnetic field, in Gauss or Tesla.

EPR spectroscopy is very sensitive to environmental factors and small perturbations in magnetic field. Slight variability may occur between the actual magnetic fields in different machines. For easier comparison between spectrometers, the horizontal axis of spectra is often reported in *g*-values, as done here. A sample of known *g*-value is used to standardize between machines. However, spectra are may also be reported in the machine's reported magnetic field. For ease of comparison with these spectra, spectra in Gauss ( $1 \text{ G} = 1 \times 10^{-4} \text{ Tesla}$ ) and *g*-values not provided above are included here.



**Ian R. Price**  
[irprice210@gmail.com](mailto:irprice210@gmail.com)  
(717) 512-6563

Permanent/Home Address:  
7293 Olde Mill Rd.  
Harrisburg, PA 17112  
(717) 657-1950

Penn State Address:  
600 E. Pollock Rd.  
Nittany Apt. 4501  
State College, PA 16801

**Education:**

The Pennsylvania State University, Schreyer Honors College, University Park, PA  
B. S. in Biochemistry and Molecular Biology. (Graduation May 2010).  
Cornell University, Graduate Field of Biochemistry, Molecular, and Cell Biology.  
Entering Fall 2010.

**Laboratory Experience:**

—Research Lab of Dr. John Golbeck, Biochemistry & Molecular Biology Department,  
Penn State University (<http://www.bmb.psu.edu/faculty/golbeck/golbeck.html>)  
BMB 496 (Independent Research) Student and summer undergraduate researcher. Fall  
2007-Present.

The Golbeck lab conducts several research projects in photosynthesis. The project that  
I help with

involves the coupling of a cyanobacterial photosystem I to a hydrogenase enzyme in  
order to produce dihydrogen. I've learned about the chemistry and biophysics of  
photosynthesis and am responsible for bacterial cell culture, protein purification,  
analysis of purity, and characterization including electron paramagnetic resonance  
spectroscopy and laser spectroscopy.

—PSU Animal Diagnostic Laboratory, Fall 2009. For and honors-option project on  
animal parasitism and physiology, I sat in on agricultural and wild animal necropsies 1-2  
times a week, learned diagnostic tests for intestinal parasite species, and compiled a  
record of all parasitism cases seen at the ADL in 2009.

**Other Skills/Experience:**

- Various molecular biology and biochemistry laboratory techniques
- Experience in keeping of a detailed research lab notebook
- Ability to work efficiently in a laboratory
- Some teaching experience through an assistant TA position in a biochemistry  
laboratory
- Basic working proficiency in Spanish

**Honors:**

- Penn State Schreyer Scholar
- Grier Fund Grant for undergraduate summer research, 2008

-Berg Fund Grant for undergraduate summer research, 2008

-Eagle Scout

**Other activities:**

-Springfield Thon, 2007-present (Thon is the largest student-run philanthropic organization in the world. It raises money for children with cancer and their families and culminates in a dance marathon, "THON" every year, which is a major event at Penn State. See [www.springfieldthon.com](http://www.springfieldthon.com))

-“Cali Conquerors” Relay for Life Team, 2006-2008

Relay for Life raises money on a national scale for cancer research.

-Volunteer with Centre County PAWS, Summer 2009

PAWS (Progressive Animal Welfare Society) is a national organization that shelters, fosters, and provides spay/neuter clinics for animals.

-Penn State Ballroom Dance, 2008

-PSU Center for Performing Arts Back-of-Stage crew (set-up, lights, strike, and other jobs for various events at the Eisenhower Auditorium or Schwab Auditorium at Penn State.)